

Coaxial End-Launched and Microstrip to Partial H-Plane Waveguide Transitions

Kevin H. Kloke, Johan Joubert, *Senior Member, IEEE*, and Johann W. Odendaal, *Senior Member, IEEE*

Abstract—Conventional rectangular waveguides are commonly used for high power and other microwave and millimeter wave applications. Their use at lower frequencies has been limited by their bulky nature. A new type of compact waveguide called a partial H-plane waveguide has previously been proposed that has only one quarter of the cross sectional area of a conventional waveguide. However, only limited information relating to the feeding of such waveguides is available. This paper presents two types of transitions to partial H-plane waveguides from the coaxial and microstrip transmission mediums. Additionally, in the coaxial case the transition is end-launched to offer collinear properties. The development of both transitions is discussed and optimized designs presented with simulated and measured results over H-band (3.95–5.85 GHz).

Index Terms—Coaxial to waveguide transition, microstrip to waveguide transition, partial H-plane waveguide transition.

I. INTRODUCTION

Often in microwave systems that employ waveguides there exists a need at some point to transition to and from waveguide and other common transmission mediums. The establishment of well defined end-launched coaxial and microstrip solutions could facilitate more wide spread use of the compact partial H-plane waveguide [1] in two ways. Firstly there only exists very limited information on partial H-plane waveguide to coaxial adapters, therefore this research will provide a well defined transition structure for the first time. Secondly since the coaxial transition is end-launched it provides collinear advantages over the probe feeds which have been previously used [2]–[5]. An example advantage is removing the need for connectors and cables on the radiating face of slot radiators, which could prevent the pattern degradation seen in [5]. In addition the microstrip adapter is also developed to enable close integration with other planar microwave components such as integrated circuits.

The first published information related to coaxial to partial

H-plane waveguide adapters was published in 2005 [2] where it was mentioned that a probe was inserted into a rectangular cut-out in the H-plane vane approximately a quarter wavelength from the end of the waveguide. The probe adapter was mentioned again in [3] with geometry and dimensions given in 2006 [4]. Fig. 1 shows the geometry given in a photo

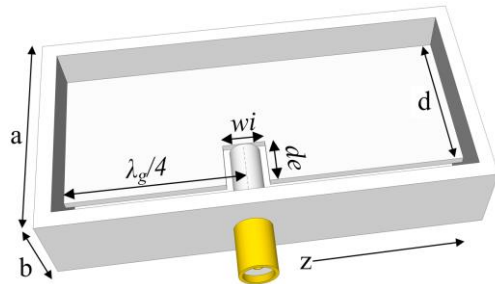


Fig. 1. Previously used probe adapter geometry (a : 23.8 mm, b : 12.0 mm, d : 20.2 mm and H-plane vane thickness 0.1 mm).

in [4] with dimension definitions.

The adapter was optimized using a commercial full wave simulator (CST Microwave Studio) where the H-plane vane cut-out width w_i and depth d_e were varied to minimize the insertion and maximize the return losses [4]. The dimensions a and b in the figure define the width and height of the waveguide, z denotes the propagation direction for context. The partial H-plane waveguide is a rectangular waveguide with a reduced height that is transversely folded flat once [1]. By unfolding the partial H-plane waveguide in Fig. 1 one can easily verify that the probe feed described above is equivalent to the classical probe feed [6] that is used in conventional rectangular waveguides.

Given the dimensions in [4] the existing probe adapter was simulated in CST MWS and an ideal waveguide port was used as the second port to facilitate simulating the insertion loss [7]. From the simulated results in [7] it can be seen that the existing probe adapter exhibits narrow band behavior around 5 GHz, which was suitable for the narrow band filter application in [4]. However a wider band transition structure is desirable for more general purpose use.

The authors presented an initial design of the end-launched coaxial to partial H-plane waveguide transition in [8]. The final version discussed in this paper achieves significantly improved performance over the entire band of interest and has been verified through measurements [8]. This paper focuses on the development of a practical end-launched coaxial and a microstrip to partial H-plane waveguide adapters with similar or larger achievable bandwidths compared to conventional

This work was supported in part by the National Research Foundation (NRF) of South Africa.

K.H. Kloke is with the Department of Electrical, Electronic and Computer Engineering, University of Pretoria, Pretoria 0002, South Africa and also with the CSIR Defence, Peace, Safety and Security, Pretoria 0001, South Africa. (e-mail: kkloke@csir.co.za).

J.W. Odendaal and J. Joubert are with the Centre for Electromagnetism, University of Pretoria, Pretoria 0002, South Africa.

rectangular waveguide probe feed adapters. The development of the coaxial transition is discussed in section II, whilst the microstrip transition is discussed in section III, and lastly a conclusion is presented in section IV.

II. END LAUNCHED COAXIAL TO PARTIAL H-PLANE WAVEGUIDE TRANSITION

The end-launched transition was developed following an iterative process where the transition geometry was incrementally updated until it achieved the desired performance. A specification of a -20 dB reflection coefficient and 0.5 dB insertion loss over the entire H-band (3.95–5.85 GHz, also known as G-band [9]) was used to ensure that the resulting design would be suitable for general purpose applications. H-band was selected to facilitate comparison with the previously used probe adapter, thus the waveguide dimensions (a , b and d) used are the same as those in Fig. 1.

A. Coaxial Transition Development

The E-field in a partial H-plane waveguide is at a maximum at the edge of the H-plane vane [1], hence the location of the probe in the existing transition in Fig. 1. Therefore it is desirable to identify a suitable conventional rectangular waveguide end-launcher that has all of its geometry located along the centre-line of the waveguide. The L-shaped loop [10] is such a geometry that lends itself well to the partial H-

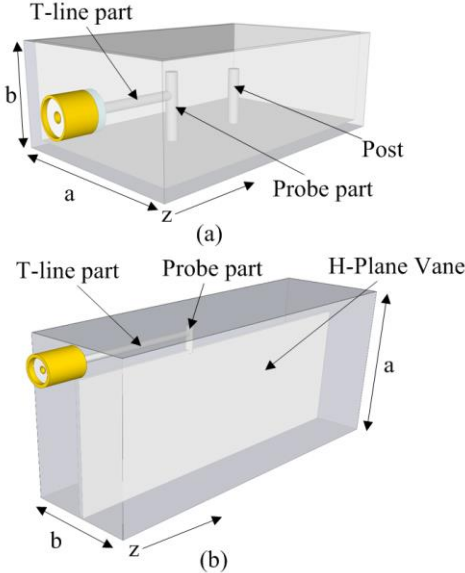


Fig. 2. L-shaped loop in rectangular (a) and partial H-plane (b) waveguides. Note, not to scale, the cross-sectional area of (b) is a quarter of that in (a).

plane waveguide case as shown in Fig. 2.

The L-shaped loop transition does not necessarily require the post for operation [10] and it is only used when wider bandwidths are required from a doubly tuned structure [11]. Note that the probe part of the transition in both the rectangular (a) and partial H-plane (b) waveguides in Fig. 2 is located where the E-field is a maximum in the respective waveguides. The operation of the L-shaped loop in rectangular waveguides is explained by the Probe Coupling Model in [10] where the L-shaped loop geometry is broken into two parts, namely the transmission line (T-line part in Fig. 2) and probe

part. A match can be achieved using three different methods, firstly the L-shaped loop can be move slightly off the centre line [10], secondly the T-line part can be extended slightly beyond the probe part [12] and lastly the contact position of the transmission line and probe parts can be varied up and down the probe's length to achieve a match [11]. The varied contact matching technique is used as all of its geometry lie along the centre line of the waveguide and it can achieve a wider bandwidth compared to the extended T-line method [7].

The prototype transition geometry shown in Fig. 2(b) was optimized for minimum reflection coefficient over the band using the CST MWS multivariable optimizer and achieved a worst case reflection coefficient of -12.1 dB over the entire band. Since the distance between the H-plane vane and side wall is quite small, a cut-out or notch in the vane can allow for a longer probe part of the loop (as in Fig. 1) which is required to achieve resonance. The addition of a cut-out and longer probe which is much closer to resonance to the prototype transition results in a worst case reflection coefficient of -14.5 dB over the band after optimization.

The next addition to the geometry was a matching section between the end-launched SMA connector and probe. Since the T-line part of the feed geometry is similar to a trough transmission line [13] the characteristic impedance of the T-line can be varied by changing the distance between the side wall and centre conductor. Therefore an impedance matching section can be introduced through the addition of a bend in the T-line. The first section of the transmission line can be kept at 50Ω to ensure continuity through the waveguide wall, whilst the second part (*Probe feed* in Fig. 3) can have a different characteristic impedance to facilitate impedance matching.

After optimizing the updated geometry the worst case in band reflection coefficient was -15.5 dB. Whilst the improvement achieved through the addition of the matching section is minimal it is required to maximize the performance achieved with the final addition of a tuning post as shown in

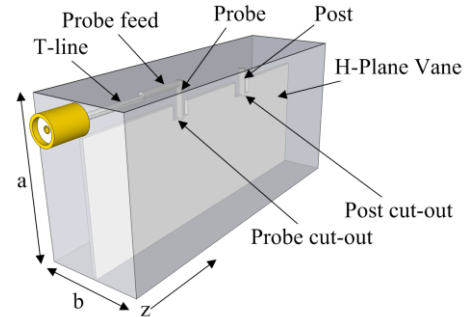


Fig. 3. Final end-launched transition geometry with the addition of a tuning post with associated post cut-out.

Fig. 3.

The addition of a tuning post makes the structure doubly tuned with two resonances resulting in two deep notches in the reflection coefficient at two different frequencies (since the length and positions of the probe and tuning post are different). Note that the tuning post, similar to the probe, does not short against the waveguide side wall.

The addition of the tuning post significantly improves the simulated reflection coefficient which is -20.38 dB and the insertion loss is 0.05 dB (see Fig. 5) which is acceptable for general purpose use.

B. Final Design Summary

A parameter study was conducted on the final design to determine which parameters affect the real or imaginary parts of the impedance and the insertion and return losses and therefore influencing the achievable bandwidth. The results from the parameter study are summarized in Table I [7].

TABLE I
END-LAUNCHED COAXIAL TRANSITION PARAMETER STUDY SUMMARY

Parameter	Optimum value (mm)	Sensitivity
SMA offset	1.34	High
T-line length	8.90	Moderate
Probe feed offset	1.13	Extreme
Probe position	22.13	Extreme
Probe cut-out depth	2.24	Insensitive
Probe cut-out width	1.93	Moderate
Probe and Post diameters	1.20	Moderate
Probe end gap	0.50	Insensitive
Post position	31.24	High
Post cut-out depth	2.35	Insensitive
Post cut-out width	1.92	Insensitive
Post end gap	0.52	Moderate

The sensitivities are classified as either insensitive, moderately sensitive, highly sensitive, or extremely sensitive. The sensitivities mainly refer to the reflection coefficient as the insertion loss is insensitive to most parameters. The parameters in Table I refer to the geometry in Fig. 3, where:

- *SMA offset* refers to the distance between the centre of the SMA connector and waveguide side wall. Larger values decrease the real component of the input impedance and vice versa.
- *Probe feed offset* is the offset between the centre of the probe feed and waveguide side and forms the matching section.
- *Probe position* and *Post position* are the distances between the shorting wall and the probe and post respectively. These distances set the lower and higher resonant frequencies respectively.
- *Probe cut-out width*, *Probe cut-out depth*, *Post cut-out width* and *Post cut-out depth* respectively refer to the dimensions of the cut-out for the probe and post in Fig. 3 (width and depth defined in Fig. 1).
- *Probe end gap* and *Post end gap* refer to the small air gap that exists between the waveguide side wall and ends of the probe and post. These values were limited to be greater than 0.5 mm to facilitate power handling in the order of a few watts.

Note that the most sensitive parameters are the *probe feed offset* (matching section) and *probe position*.

C. Measured Results

A hardware prototype of the end-launched coaxial transition was realized in the back-to-back configuration to facilitate comparison with the simulated results. The prototype was realized with 6 mm side walls, a 1 mm thick partial H-plane vane and a total internal length of 237 mm. A vane thickness of 1 mm was used over the 0.5 mm [3]-[5] thickness previously used as it provided more mechanical stability and did not negatively influence the full band performance of the

waveguide. A photo of the prototype is given in Fig. 4.

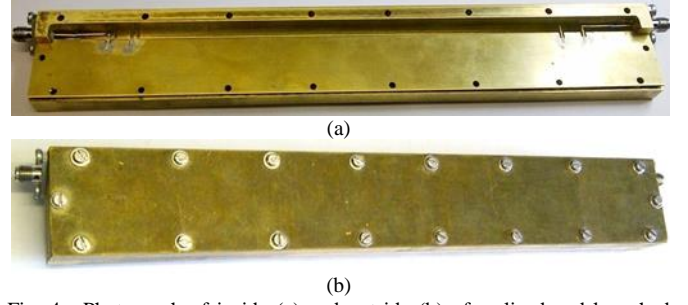


Fig. 4. Photograph of inside (a) and outside (b) of realized end-launched coaxial transition to partial H-plane waveguide.

Note that the joints between the T-line, probe feed and probe were solder joints. Similarly the probe and post were attached to the partial H-plane vane by solder joints. The use of these solder joints is believed to be the primary cause of the differences between simulated and measured results.

The measurement setup is shown in Fig. 5 below, a Rohde & Schwarz ZVA-40 vector network analyzer was used to capture the measured results.

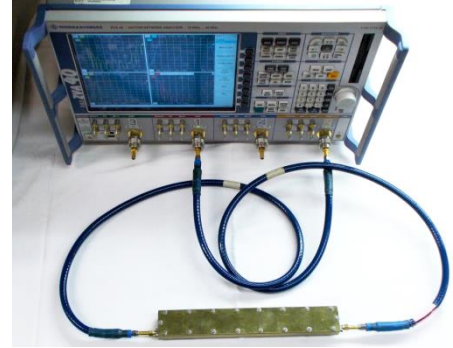


Fig. 5. Measurement setup with prototype under test.

The back-to-back measured and simulated results for the realized prototype are given in Fig. 6.

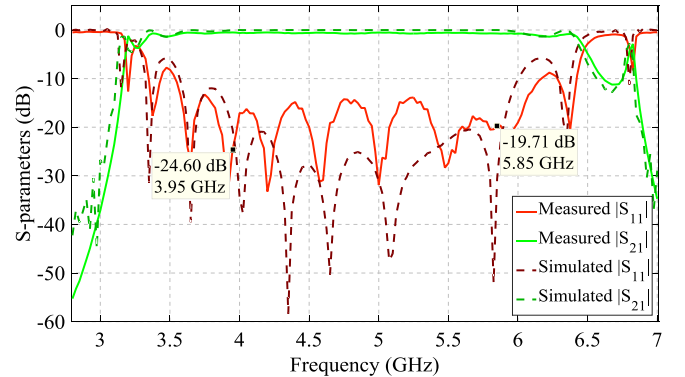


Fig. 6. End-launched coaxial transition back-to-back measured and simulated results.

D. De-embedded Single Adapter Results

The back-to-back measured results presented above contain the combined effect of the two adapters on either end of the prototype and waveguide section between them. The process of extracting the approximate single ended response from the combined back-to-back is referred to as de-embedding as the single ended response is so-called “embedded” in the total response [14]. Equation (1) represents the realized prototype

containing the embedded single adapters on either end of the waveguide using transfer scattering matrices (T-parameters) [15], (also known as chain scattering parameters) [16].

$$[T_{VNA}] = [T_{adapter1}][T_{line}][T_{adapter2}] \quad (1)$$

The T-parameters are similar to the S-Parameters in that they also relate the voltages of waves reflected and transmitted at ports. However they can easily be cascaded to determine the result of a cascaded network (such as the back-to-back case), which is not possible to do directly with S-parameters [15]. Assuming that the two adapters have identical responses and that the intermediately section of waveguide is lossless the approximate single adapter results can be obtained using (1). Additionally the propagation constant used in the de-embedding was simulated using CST MWS and assumed to be similar to that of the realized prototype. The approximate single adapter response given the assumptions above is shown below in Fig. 7.

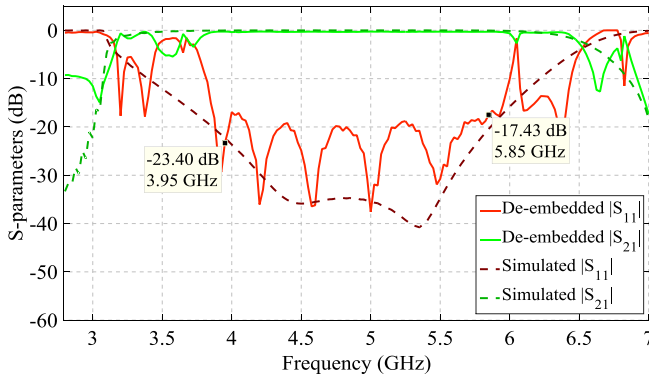


Fig. 7. De-embedded measured and simulated single adapter S-parameters.

The worst case in-band reflection coefficient is -17.4 dB and the insertion loss is 0.75 dB.

III. MICROSTRIP TO PARTIAL H-PLANE WAVEGUIDE TRANSITION

As in the coaxial case the microstrip transition was developed following an iterative process where the transition geometry was incrementally updated until it achieved the desired performance.

A. Microstrip Transition Development

Similarly to the coaxial case a suitable conventional rectangular waveguide transition structure is identified for use in the partial H-plane waveguide case. The integrated broadside microstrip adapter was selected as the feed structure to adapt to the partial H-plane scenario due to large potential bandwidths of up to 40% [17] and simplicity as the entire feed structure and H-plane vane may be integrated on a single microstrip substrate. The integrated broadside microstrip probe used in conventional rectangular waveguides (see Fig. 8(a)) can be adapted for the partial H-plane geometry by bending the conventional waveguide like a horseshoe (see Fig. 8(b)). Via stitching is used to close the edge of the integrated vane inside the waveguide. An SMA connector is included in

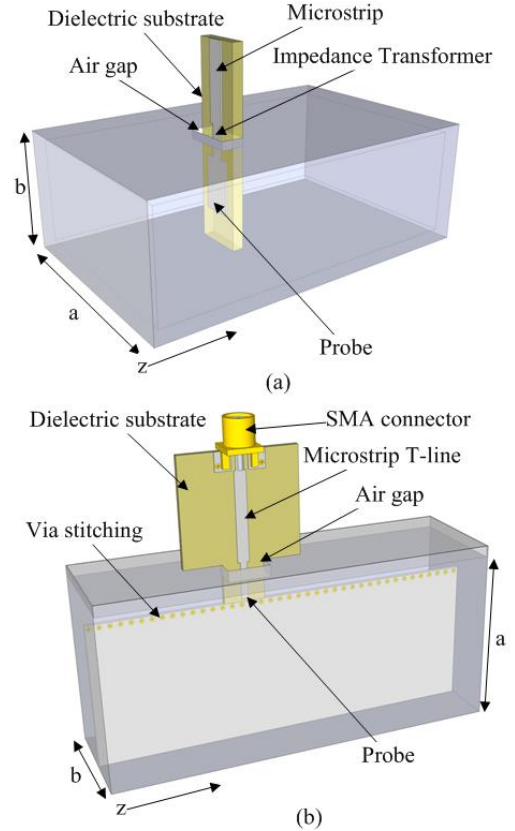


Fig. 8. Microstrip probe in rectangular (a) and partial H-plane (b) waveguide. Note, not to scale, the cross-sectional area of (b) is a quarter of that in (a).

the partial H-plane waveguide model in Fig. 8(b) to facilitate measurements with a vector network analyzer (VNA). Rogers RO4003C with a thickness of 0.813 mm was selected as the microstrip substrate.

The probe feed geometry given in Fig. 8(b) consists of a 50Ω microstrip line up to the waveguide's external wall and a probe integrated onto the same substrate going through a hole in the waveguide's side wall. The air gap above the substrate in Fig. 8(b) and the substrate width going through the waveguide wall were optimized to be as small as possible without negatively affecting the return loss. The probe width and position from the shorting wall were also optimized using CST MWS for the maximum return loss over the entire band. The optimized initial microstrip transition geometry in Fig. 8(b) achieved a worst case in-band reflection coefficient of -8.4 dB, which is not sufficient for general purpose use.

As with the coaxial prototype, the first update to the initial transition geometry is a cut-out to facilitate a longer *probe* section in Fig. 8(b). The extended probe protrudes into the vane but does not make electrical contact with the vane. The integrated substrate of the feed and vane ensures mechanical stability and accuracy. The updated geometry with the addition of the probe cut-out achieved a reflection coefficient of better than -19.6 dB over the entire band after optimization.

An external (to the waveguide) matching section was added to further reduce the reflection coefficient. With this addition the prototype transition achieved a worst case in band reflection coefficient of -21.9 dB. Although not as significant as the previous addition to the prototype this step will enable the next addition of a tuning post to yield vastly superior wideband performance. Fig. 9 gives the final microstrip

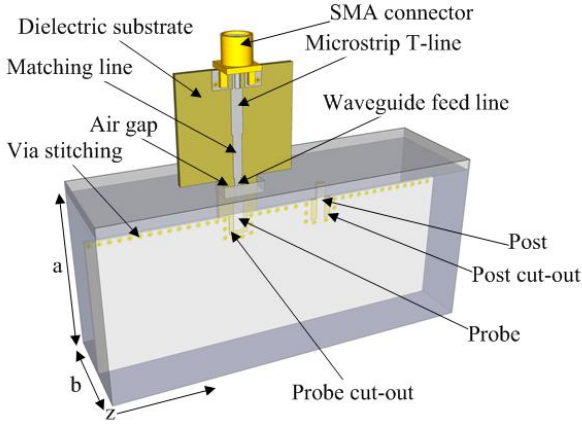


Fig. 9. Final microstrip geometry with the addition of a tuning post.

geometry, as in the coaxial case the post does not short against the side wall.

The addition of a post is strictly not necessary as the microstrip adapter already had satisfactory results. However this addition yields a maximum reflection coefficient of -32.0 dB and insertion loss of 0.2 dB (see Fig. 12), which outweighs the additional complexity having the addition of a post.

B. Final Design Summary

As with the coaxial transition a parameter study was conducted on the final microstrip design to determine which parameters affect the achievable bandwidth. The results from the parameter study are summarized in Table II [7].

TABLE II
MICROSTRIP TRANSITION PARAMETER STUDY SUMMARY

Parameter	Optimum value (mm)	Sensitivity
Transmission line width	1.78	Moderate
Matching line length	5.02	Insensitive
Matching strip width	1.61	High
Feed-line width	0.71	Extreme
Feed-line gap width	3.59	Insensitive
Feed-line air gap	2.00	Insensitive
Probe position	19.40	Extreme
Probe cut-out depth	2.98	High
Probe cut-out width	1.76	Moderate
Probe width	1.15	Moderate
Post position	29.24	Moderate
Post cut-out depth	4.46	Moderate
Post cut-out width	3.51	Insensitive
Post width	1.60	Moderate
Post end gap	0.54	Moderate

The parameter names in Table II refer to the final geometry in Fig. 9, where:

- *Matching line length* refers to the length of the matching section with width, *Matching strip width*. Longer lengths decrease the return loss at mid-band at the expense of the band edges.
- *Feed-line gap width* and *Feed-line air gap* define the width and height of the air gap that exists above the substrate passing through the waveguide side wall respectively.
- *Probe position* and *Post position* are the distances

between the shorting wall and the probe and post in the figure respectively. As with the coaxial case the *Probe position* controls the lower resonance and the *Post position* the higher resonance frequency.

Note that the most sensitive parameters in the design are the *Feed-line width* (microstrip width going through the waveguide side wall) and *Probe Position*.

C. Measured Results

As with the coaxial case a hardware prototype transition was realized in the back to back configuration to facilitate the acquisition of measured results. A photo of the inside and outside of the realized prototype is given in Fig. 10.

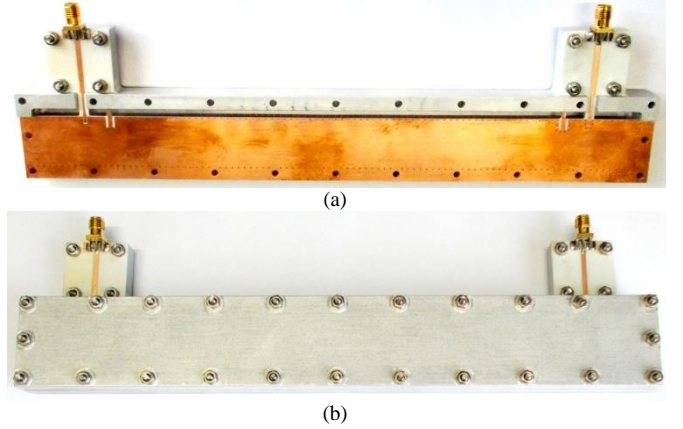


Fig. 10. Photograph of inside (a) and outside (b) of realized microstrip transition to partial H-plane waveguide.

The back-to-back measured and simulated results for the realized prototype are given in Fig. 11.

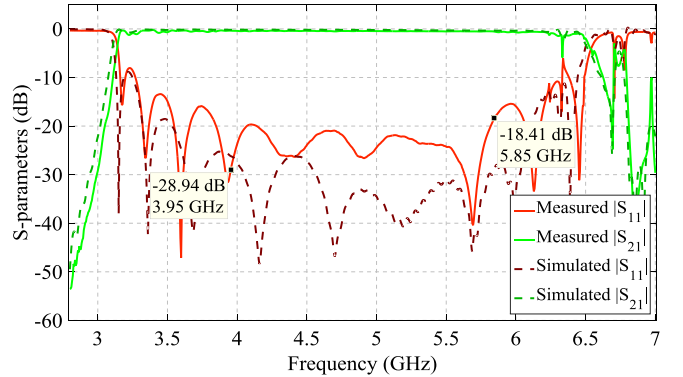


Fig. 11. Microstrip transition back-to-back measured and simulated results.

D. De-embedded Single Adapter Results

Using the de-embedding technique and assumptions previously discussed the approximate single adapter results shown in Fig. 12 were obtained.

The worst case in-band reflection coefficient is -23.7 dB and the insertion loss is 0.27 dB, which correspond well with the simulated results. The two sharp responses in the measured S_{11} at approximately 6.3 GHz are caused by differences between the simulated propagation constant used in the de-embedding and the actual propagation constant in the realized prototype. Specifically, these two de-embedding artifacts are the result of the difference in frequency where the second

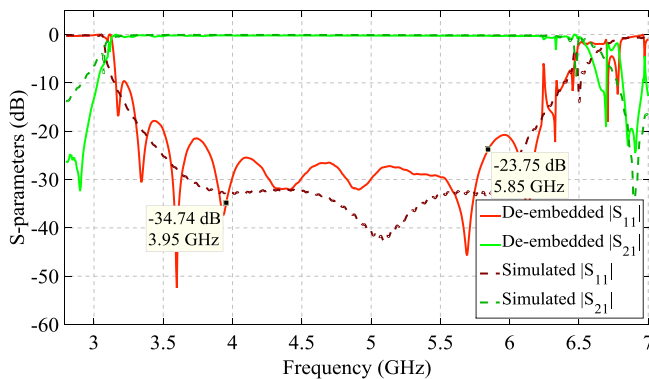


Fig. 12. De-embedded measured and simulated single adapter S-parameters.

mode starts propagating. Since this is outside of the band of interest (3.95–5.85 GHz) it does not affect the results.

IV. CONCLUSION

The development and realization of two types of transitions between partial H-plane waveguides were discussed, namely the end-launched coaxial and microstrip transitions. Hardware prototypes were realized for each design in back-to-back configuration to facilitate measurements of insertion loss and reflection coefficient of the realized transitions. De-embedding techniques were used to approximate the single adapter responses from the back-to-back measurements. The measured results of the end-launcher and microstrip transitions compare favorably with the simulated results and validate the designs.

REFERENCES

- [1] D.W. Kim and J.H. Lee, "A partial H-plane waveguide as a new type of compact waveguide," *Microwave and Optical Technology Letters*, Vol. 43, No. 5, pp. 426-428, Dec. 2004.
- [2] D.W. Kim and J.H. Lee, "Partial H-Plane Filters with Partially Inserted H-Plane Metal Vane," *IEEE Microwave and Wireless Components Letters*, Vol. 15, No. 5, pp. 351-353, May 2005.
- [3] D.J. Kim, J.G. Lee, K.D. Kim, and J.H. Lee, "Quarter Wavelength Resonator Partial H-plane Filter," in *36th European Microwave Conference*, Manchester, UK, 2006, pp. 991-993.
- [4] D.W. Kim, D.J. Kim, and J.H. Lee, "Compact Partial H-Plane Filters," *IEEE Transactions on Microwave Theory and Techniques*, Vol. 54, No. 11, pp. 3923-3929, Nov. 2006.
- [5] D.J. Kim and J.H. Lee, "Compact Resonant Slot Array Antenna Using Partial H-Plane Waveguide," *IEEE Antennas and Wireless Propagation Letters*, Vol. 9, pp. 530-533, 2010.
- [6] R.F. Harrington, "Microwave Networks," in *Time-Harmonic Electromagnetic Fields*, New York: McGraw-Hill, 1961, pp. 425-428.
- [7] K. H. Kloke, "End-launched Coaxial and Microstrip to Partial H-Plane Waveguide Adapters," M.Eng. dissertation, Dept. Elect., Electron. and Comput. Eng., Univ. of Pretoria, Pretoria, South Africa, 2014.
- [8] K.H. Kloke, J. Joubert and J.W. Odendaal, "End-launched coaxial to partial H-plane waveguide adapter," presented at the IEEE International Symposium on Antennas and Propagation and USNC/URSI Radio Science Meeting, Chicago, IL, 8-14 July 2012, pp. 1.
- [9] D.M. Pozar, "Appendix I," in *Microwave Engineering*, 3rd ed., New York: Wiley, 2005, pp. 688.
- [10] S.M. Saad, "A More Accurate Analysis and Design of Coaxial-to-Rectangular Waveguide End Launcher," *IEEE Transactions on Microwave Theory and Techniques*, Vol. 38, No. 2, pp. 129-134, Feb. 1990.
- [11] V. Galdi, G. Gerini, M. Guglielmi, H.J. Visser, and F. D'Agostino, "CAD of Coaxially End-Fed Waveguide Phased-Array Antennas," *Microwave and Optical Technology Letters*, Vol. 34, No. 4, pp. 276-281, Aug. 2002.

- [12] B.N. Das and G.S. Sanyal, "Coaxial-to-waveguide transition (end-launcher type)," *Proceedings of the Institution of Electrical Engineers*, Vol. 123, No. 10, pp. 984-986, Oct. 1976.
- [13] R.M. Chisholm, "The Characteristic Impedance of Trough and Slab Lines," *IRE transactions on Microwave Theory and Techniques*, Vol. 4, No. 3, pp. 166-172, July 1956.
- [14] R.F. Bauer and P. Penfield, "De-Embedding and Unterminating," *IEEE transactions on Microwave Theory and Techniques*, Vol. 22, No. 3, pp. 282-288, Mar. 1974.
- [15] M.N. Sadiku and C.M. Akujuboi, "S-Parameters for Three and Four Cascaded Two-Ports," in *IEEE Southeast Con 2004 proceedings*, 2004, pp. 410-412.
- [16] D.A. Frickey, "Conversion Between S, Z, Y, h, ABCD, and T Parameters which are Valid for Complex Source and Load Impedances," *IEEE transactions on Microwave Theory and Techniques*, Vol. 42, No. 2, pp. 205-211, Feb. 1994.
- [17] Y.C. Shih, T.N. Ton, and L.Q. Bui, "Waveguide-To-Microstrip Transition for Millimeter-Wave Applications," in *IEEE MTT-S International Microwave Symposium Digest*, Vol. 1, 1988, pp. 473-475.



Kevin H. Kloke received the B.Eng. and M.Eng. degrees in electronic engineering from the University of Pretoria, Pretoria, South Africa in 2008 and 2014 respectively.

Since January 2009, he has been with the Council for Scientific and Industrial Research (CSIR), Defence, Peace, Safety and Security (DPSS), Radar applications research group, Pretoria. His research interests include partial H-plane waveguides and design and development of antennas for airborne radar applications.



Johan Joubert (M'86–SM'05) received the B.Eng., M.Eng. and Ph.D. degrees in electronic engineering from the University of Pretoria, Pretoria, South Africa, in 1983, 1987 and 1991 respectively.

From 1984 to 1988 he was employed as a Research Engineer at the Council for Scientific and Industrial Research, Pretoria. In 1988, he joined the Department of Electrical and Electronic Engineering at the University of Pretoria, where he is currently a Professor of Electromagnetism. His research interests include antenna array design and computational electromagnetism.



Johann W. Odendaal (M'90–SM'00) received the B.Eng., M.Eng., and Ph.D. degrees in electronic engineering from the University of Pretoria, Pretoria, South Africa, in 1988, 1990, and 1993, respectively.

From September 1993 to April 1994, he was a Visiting Scientist with the ElectroScience Laboratory at the Ohio State University. Since May 1994, he has been with the University of Pretoria, where he is currently a Full Professor. His research interests include electromagnetic scattering and radiation, compact range measurements, and signal processing. He is also Director of the Centre for Electromagnetism at the University of Pretoria.